The Electrode System in Impedance-Based Ventilation Measurement

Shen Luo, *Student Member, IEEE,* Valtino X. Afonso, *Student Member, IEEE,* John G. Webster, *Fellow, IEEE,* and Willis J. Tompkins, *Fellow, IEEE*

***Abstract*—In this paper, we determined which electrode types, sizes, and locations were best suited for impedance-based ventilation measurement. Optimal electrodes provide high signal-to-(motion) artifact ratio (SAR) and reliability by meeting the following criteria: 1) low baseline impedance, 2) high adhesion, 3) good physical stability, 4) large effective area, 5) thin with high flexibility. We compared 14 electrodes from two main groups: adhesive-gel and conductive rubber electrodes. Adhesive-gel electrodes are easy to apply, make good body contact, and do not slip during the course of an experiment. We found that higher SAR's are obtained when electrode area is increased by connecting several small electrodes together rather than by using a single electrode with a larger area. The peak SAR is achieved when two electrode arrays (area = 70 cm^2) are centered at the 8th intercostal spaces on opposite midaxillary lines. To determine the optimal electrode locations, we placed 32 electrodes on the trunk and recorded impedance between 171 electrode combinations on ten normal adult subjects. Based on these data, we conclude that the SAR's are highest when one electrode is placed on the midpoint between the left and right second intercostal spaces on the sternum and the other electrode is placed in the opposite position on the back.**

I. Introduction

An accurate noninvasive ventilation measurement is desired in many clinical and research situations, including apnea monitoring, ventilation monitoring in intensive care units, lung monitoring for patients suffering from respiratory diseases, and sleep studies when the breathing pattern and respiration rate as well as ECG and EEG signals are recorded. Because of convenience and practicality for long-term or home monitoring as well as the compatibility of the electrodes with ECG monitoring, impedance pneumography is the most widely used method for respiration monitoring [1].

Like many medical instruments, an impedance pneumograph is composed of two parts, an electrode system and an electronic device. The device injects a small, high-frequency, constant current through the thorax and/or abdomen through a pair of electrodes. Air volume variation in the lungs and movements, such as motion of chest wall and diaphragm, modulates the voltage drop across the body. This voltage is measured by the same electrodes (two electrode method [2]) and is directly proportional to the impedance change. An inherent problem with this technique is that it is sensitive to any movement; undesired motion often results in large amplitude artifacts within the current pathway giving rise to problems from motion artifact [1], [3]–[5]. In fact, today's impedance-based ventilation systems often fail to identify whether the signals are from respiratory efforts and body motion without air flow or from normal body motion with air flow. Also they have mechanical problems [4], such as fragility of leads.

Both the electrode system and detection techniques affect the reliability of impedance-based ventilation monitoring. Unfortunately, insufficient attention has been devoted to the electrode system.

The purpose of this study was to evaluate the impact on impedance-based ventilation measurement of three important electrode characteristics: 1) type, 2) size, and 3) placement. The electrode system provides an electrochemical interface between the patient and the electronic device for both current injection and voltage sensing. The two types of electrodes primarily used for ventilation measurement are adhesive-gel electrodes and conductive-rubber electrodes. Most adhesive-gel electrodes were originally designed for electrocardiography; thus, their performance in impedance measurement needed to be evaluated. A previous study shows that the signal-to-artifact ratio (SAR) increases with electrode area [6], and the possibility of optimal electrode size needed to be investigated. Finally, for a given patient, the SAR can vary by a factor of 100 as a function of electrode placement; thus optimal electrode placement needs to be determined. This study addresses these needs, and its results provide some insight for designing an improved apnea monitor.

II. Materials and Methods

A. Data Acquisition

During our previous studies in electrical impedance tomography (EIT) [7], we developed a system for recording impedance signals either from one channel for up to 10 days or from 32 channels for up to 8 h. The system consists of interface electronics and a Macintosh II computer. The device includes two parts, the current output and the voltage measurement. Each of 32 independent voltage-controlled current sources produces sinusoidal

Manuscript received January 6, 1992; revised June 8, 1992. This work was supported by NSF Grant BCS-90127820.

The authors are with the Department of Electrical and Computer Engineering, University of Wisconsin, Madison, WI 53706.

IEEE Log Number 9203402.

current up to 5 mA (rms) at a frequency of 50 kHz over a load range of 0–850 Ω. A time-sharing method is employed to ensure that only one channel is active at a time. Thirty-two multiplexed voltage buffers measure the voltage between any pair of electrodes according to the software-controlled configuration. Then the voltages are demodulated, filtered, and amplified. The voltage signals include a small ac component due to impedance variation with time and a large dc component which is proportional to the baseline impedance between that pair of electrodes [8]. To use the full dynamic range of the analog-to-digital converter (ADC) for the time-varying parts of the signals, a hardware subtracter removes the dc components. As controller and processor, the computer connects to the device through a signal conversion and timing board (National Instruments NB-MIO-16) and a parallel I/O board (National Instruments NB-DIO-24).

The software controls the hardware to acquire a maximum of 32 channels of ventilation signals. The electrode combination for each channel can be set by specifying the positive and negative nodes for each current source. The voltage is measured from the same electrode combination. The sampling rate is programmed at 3 Hz per channel for a 32-channel configuration.

The effect of sampling rate on SAR was observed by performing preliminary experiments using the test protocol defined in the following section. The SAR from data obtained at a sampling rate of 60 Hz, SAR_60, was compared to that of the same data sampled at 3 Hz (sampled every 20 points in the 60-Hz sampled data), SAR_3. The maximal SAR error of SAR_3 with respect to SAR_60 over two experiment trials for each of the subjects was less than 9%. The test protocol did not result in SAR measurements which varied significantly with sampling rate. Since a part of this study is to determine best electrode locations, we acquired data from as many channels as the software was designed for. Data storage limits then restricted us to using a sampling rate of 3 Hz. Room temperature was kept high to avoid introduction of high frequencies in the signal caused by shivering.

The software also allows a real-time display of any of the 32 channels, storage and retrieval of the ventilation signals, and relevant information about the patient being monitored and about the experimental setup.

B. Test Protocol

We have developed a test protocol which defines the pace and pattern of breathing and movement for comparing electrode types, sizes, and placements under the same test conditions (see Appendix). We performed a comprehensive study of the electrode system, according to the definitions in the protocol.

C. Comparing Electrode Types

To find a suitable impedance measurement electrode for the apnea monitor, we tested two main groups of electrodes for respiratory impedance measurements: adhesive-gel electrodes and conductive rubber electrodes. Our tests included a study of methods on how to attach nonstick electrodes to the skin. We selected twelve commercial electrodes for our study: the Siemens Burdick Dispos-A-Trode/2, 3M Red Dot 2269T, Sentry Silver Sircuit 1021, Sentry Silver Sircuit 1022, Biotab-2, Siemens Burdick Signa II 047029, Graphic Controls Q-Trace 5400, Sentry Silver Sircuit 1071, 3M Tenzcare rubber 6225, LecTec SynCor S-101, Sentry rubber 3425, and Marquette defibrillator 400317-001. We also tested two custom-designed electrodes. One called Custom Compound was developed for EIT [9]. A compound electrode consists of an inner electrode surrounded by an outer electrode on a common support. In our studies, we connected both inner and outer electrode together as a simple plate electrode. Another was developed by removing the gel layers of both a Signa II (Siemens Burdick) and Red Dot 2269 (3M) then attaching Red Dot's adhesive-gel to Signa II's tin foil back in order to compare different gels under the same size.

We measured the face-to-face impedances and electrode-body impedances (or transthoracic-plus-electrode impedances) at room temperature (25°C). To find face-to-face impedance, we pressed two of the same electrodes together for 5 s, waited 50 s, then measured the impedance. We applied 1% saline between the rubber electrodes. Results for each electrode are the average of four tests.

The experiment for measuring transthoracic-plus-electrode impedances was performed on four normal male subjects and the results were averaged. The skin was prepared by shaving any hair if present, and the two electrodes were respectively placed at the approximate levels of the 8th intercostal spaces on the midaxillary lines of both sides. Similarly, we applied 1% saline on the rubber electrodes. We attached Sentry rubber 3425 nonstick electrodes to the body using a customized stretch band and Velcro®, a commercial Stress Test Shirt, or tape.

D. Comparing Electrode Sizes

In order to study the relationship between electrode impedance and electrode size, we first employed the same methods described previously to measure the face-to-face and electrode–body impedances of three kinds of electrodes: Marquette defibrillator, Sentry rubber and Burdick Signa II. Electrode sizes ranged from 14 to 108 cm^2. Then we recorded the SAR's with the area change.

We used two approaches to change electrode size. For the large defibrillator electrode, we changed the area by dividing 108 cm^2 into six 18-cm^2 pieces. During the experiment, we pressed the large electrode on the location, then measured SAR from large to small area by successively cutting and removing pieces. For the small electrodes, 16-cm^2 Sentry rubber and 7-cm^2 Signa II, we respectively connected several together with wires to form one large-area electrode, then measured them from large to small size by cutting wires and removing electrodes. Similarly, we connected six 18-cm^2 pieces cut from a

Marquette defibrillator electrode to construct a new large area electrode. However, the results were significantly different, as we will discuss later.

The experiment was performed on three normal male subjects. The two electrodes were respectively centered at the approximate levels of the 8th intercostal spaces on the midaxillary lines of both sides.

Again, we applied 1% saline on the rubber electrodes. We used four stretch bands to keep the Sentry rubber array in place.

E. Comparing Electrode Placements

Electrode location on the body is one of the main factors which influences the quality of signal acquisition. In order to find the relationship between the SAR and the electrode placement, and also the best and worst location(s), we placed 32 electrodes evenly around the body trunk at four levels (Fig. 1). There exist 496 (16 × 31) pairs of electrode combinations. For our system, it would have been time consuming to repeat each experiment 16 times on each subject to acquire data from all combinations. Therefore, we performed a preliminary study to reduce the experiment time.

We first selected four subjects with different ages and weights. We performed a series of experiments to find which locations were best. The results suggested that the Locations 6, 10, 21 and 25 had high SAR for lean subjects; Location 31 for heavy subjects and Location 0 for minimal motion artifact. Next, we performed the same test on three additional subjects to confirm the conclusion. Finally, we designated the above six locations as reference placements so that each of them together with 31 other locations formed 31 pairs of electrode locations. The regular study was based on these 171 (6 × 31–15) pairs of combinations.

We chose the low-cost Signa II as the experimental electrodes. We connected two Signa IIs (each 7 cm^2) as a 14 cm^2 electrode and soldered a connecting wire between them. Before and after soldering wires to electrodes, we kept them in the sealed containers until they were used to prevent drying out. We placed two electrodes horizontally with a space of about 3 mm between them to prevent them from touching. The ten subjects (nine males and one female) were between 24 and 59 years of age and weighed from 54 to 85 kg. We asked every subject to perform the maneuvers specified in our test protocol.

Based on our previous experiments, we note that it is impossible to find a universally best pair of electrode locations (electrode combinations) which is suitable for everyone. Electrode combinations which were best for some individual were not best for others. To compare different electrode positions, we employed four parameters based on SAR's for normal breathing (see the test protocol in Appendix). The first one is the SAR of the worst case, which is the lowest SAR value among the ten subjects for each combination. Thus for any of the ten subjects, SAR will be this value or better. In contrast, the second parameter, the SAR of the best case, is the highest SAR value among the ten subjects for each combination. The remaining two parameters, mean and standard deviation, are obtained from SAR's normalized to the maximal SAR value of 171 pairs of electrode combinations for each subject, and then calculated for each electrode combination over ten subjects.

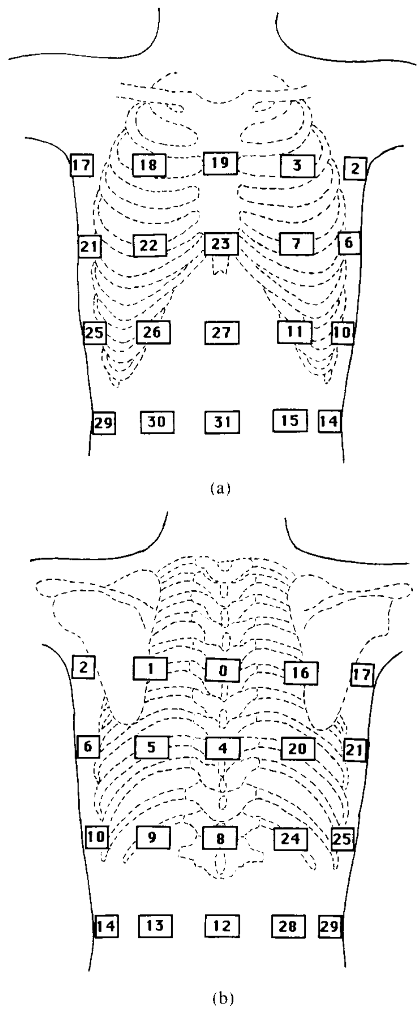

Fig. 1. Thirty-two electrode locations are evenly distributed on the thorax and abdomen, on the corners of four latitudes (horizontal levels) and eight longitudes (vertical lines) with 45° included angles. Location 19 was on the midpoint between the left and right second intercostal spaces on the sternum. This determines Level 1 and the 0° longitude. Locations 10 and 25 respectively were at the levels of the 8th intercostal spaces on the midaxillary lines of both sides on Level 3. The midline of Level 1 and 3 is Level 2. The distance between Level 3 and 4 is the same as that between Level 2 and 3. (a) Anterior view. (b) Posterior view.

III. Results and Discussion

The types, sizes, and placements of electrode systems directly affect the quality and characteristics of acquired data. A good electrode system provides high SAR and reliability by meeting the following criteria: 1) low baseline

TABLE I
EFFECTIVE AREAS, FACE-TO-FACE IMPEDANCES AND ELECTRODE–BODY IMPEDANCES FOR 14 DIFFERENT ELECTRODES AT 50 kHz

Electrodes	Area (cm²)	Face-to-Face Impedance (Ω)	Electrode-Body Impedance (Ω)
Burdick Dispos-A-Trode/2	1.3	8.9	552
3M Red Dot 2269T	2.1	353.0	681
Custom Compound	5.3	29.3	407
Sentry Silver Sircuit 1021	5.8	96.3	408
Sentry Silver Sircuit 1022	5.8	16.5	331
Biotab-2	6.7	103.6	483
Signa II's tin foil plus 3M gel	7.0	21.1	218
Burdick Signa II 047029	7.0	33.4	262
GC Q-Trace 5400	7.2	290.0	552
Sentry Silver Sircuit 1071	8.1	81.1	264
3M Tenzcare rubber 6225	9.7	138.0	345
LTC SynCor S-101	16.0	1173.9	1795
Sentry rubber 3425	16.7	27.6	193
Marquette defibrillator 400317-001	108.0	0.7	60

impedance, 2) high adhesion, 3) good physical stability, 4) large effective area, 5) thin electrode with high flexibility.

A. Electrode Types

We tested 14 different electrode types from two main categories of electrodes for respiratory impedance measurements, adhesive-gel electrodes and conductive rubber electrodes. Table I shows their effective areas, face-to-face impedances, and electrode–body impedances at 50 kHz.

A small face-to-face impedance is desirable because this impedance contributes to the total impedance measured, and any changes in this value will also be small. Moreover, the operating range of the current source for impedance measurements is limited. For our system, for example, an electrode–body impedance larger than 850 Ω at 50 kHz causes a false result due to distortion of the current waveform. Because the electrode–body impedance varies not only with electrode types and sizes, but also with electrode dryness and placement as well as skin dryness or oiliness, etc., a higher impedance has a larger risk of exceeding the current source limit. Therefore, we prefer low impedance electrodes for this purpose.

The conductive rubber electrodes have low impedance, are reusable, stable, and acceptable for hairy subjects. It is difficult, however, to make good contact between the skin and nonstick rubber electrodes and keep them from slipping. They have poor contact occasionally and slippage problems even after adding 1% saline to the electrode–skin interface (without saline they are much worse). Poor contact causes large motion artifact as shown in Figure 2. Another problem is attaching electrodes at an arbitrary location. We tried to apply a commercial elastic net Stress Test Shirt and tape to keep nonstick rubber electrodes in place. However, our results show that neither the Stress Test Shirt nor tape nor both together adequately keep nonstick electrodes in good contact or from slipping. Even employing a rather tight stretch band, we found, for

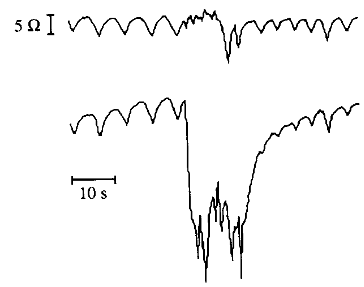

Fig. 2. The nonstick rubber electrode sometimes yields large motion artifact. The impedance signal on the top channel is obtained through two Siemens Burdick Signa II sticky electrodes (total 14 cm²) connected with wire, and that on the bottom through Sentry 3425 rubber nonstick electrode (16 cm²). We used a customized stretch band and Velcro® to attach the rubber electrodes to the skin. Both electrodes are located close to each other. The first four cycles are normal breathing signals followed by motion artifact without breathing. The subject moves the limbs according to our protocol. After that, the subject stops movement and breaths again.

a trunk with a triangular shape, that the band and electrodes slip together, especially as the upper limbs move.

To obtain a good SAR, therefore, we prefer a sticky electrode for our measurements. The impedances of different kinds of adhesive-gel electrodes vary greatly. One of the reasons is the characteristics of the gel. Comparing the original Signa II gel with 3M Red Dot 2269 gel under same size listed in Table I we find that different gels have different impedances and thus gave different interface impedances at 50 kHz.

The defibrillator electrode has excellent adhesion and low impedance at 50 kHz, but the adhesive-gel layer is so thick that it is not flexible. Of course, the large size is another problem.

Compared with the defibrillator electrodes, other adhesive-gel electrodes have less adhesion and often result in local falloff when used for more than one-half hour. Such looseness introduces artifact. In addition, all electrodes with a gel layer are unstable with temperature and humidity. When the gel layer dries, this greatly increases

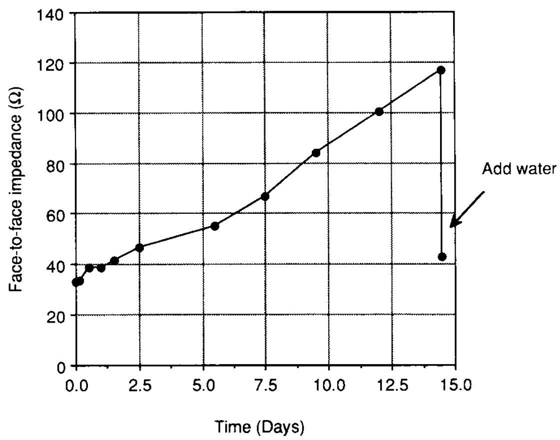

Fig. 3. The impedance of the Signa II ECG electrode increases with drying time. We opened a package of electrodes, spread them out in a drawer at about 25°C. At the times shown, we measured four pairs and averaged the results.

the face-to-face impedance (Fig. 3). If a few drops of water are added to the gel surface, the impedance recovers to a value which is slightly larger than the original, but once dried out, the electrode adhesion does not significantly increase with water.

Sentry Silver Sircuit 1021, 1022 and 1071 are adhesive-gel electrodes designed to be reused many times. These electrodes have flexible wires and a connecting pin which makes it convenient for connecting them with monitors. Also, the small gage flexible wire can prevent the electrode from peeling off compared to using a heavy clip on an electrode without wire. In addition, a small package keeps the electrodes fresh. Moreover, the electrodes have low impedance and are suitable in size for children. Its per application cost can be lowered by repeated use. This is a good design for an apnea monitor. However, there are problems. After two uses, we found that the area of the foil layer that connected to the wire at the back started to break, and the adhesive gel partially degraded.

3M Red Dot 2269T is a specially designed electrode with a carbon filament wire that is radiolucent. One terminal of the wire connects to a pin, the other attaches to a disk covered by Ag/AgCl. Although its face-to-face impedance without the wires is only 50 Ω, the pin-to-pin impedance is higher because the wire itself has a 120-Ω impedance. Also compared to other adhesive-gel electrodes, it is too sensitive to pressure for our application possibly because of the variable resistance of the ohmic connection between the Ag/AgCl film and the carbon wire.

Therefore, an electrode meeting the following requirements is desirable for use in impedance-based ventilation measurement: low baseline impedance, high adhesion, high physical stability, thin electrode with high flexibility.

B. Electrode Sizes

Table I shows that the transthoracic-plus-electrode impedances for different electrodes do not simply follow the change of face-to-face impedances. Besides electrode material, electrode size is a main factor which contributes to electrode differences. For firm attachment, some electrodes have a large conductive adhesive-gel area backed by a smaller metal electrode. For example, the effective area of a 3M Red Dot 2269T electrode is about one third of the total attaching area, and some like the Dispos-A-Trode/2 is only about one tenth. Our experiments showed that adding the two thirds conductive gel layer without direct metal backing to the 3M Red Dot electrode changed its face-to-face impedance value by only 4%. The current distributions of a small-area interface and immediate tissue are rather uneven and the current density is higher than that of a larger electrode. This results in a high voltage drop in the area. Fig. 4 shows that electrode–body impedances change more with area than do the face-to-face impedances.

Further, it is important to know the relationship between the SAR and electrode size. A previous study showed that the larger the electrode area, the higher the SAR [6]. A possible explanation is that the large area electrode has an averaging function which reduces random motion artifact. However, for defibrillator electrodes, we could not reproduce these results on two out of three male subjects [Fig. 5(a)]. After thorough observation, we found that an adhesive polymer with large area in fact imposes a restriction on the movement of the immediately underlying skin and tissues, and tends to unify originally local movement with different patterns under the coverage, such as bending and stretching. Such restriction results in skin strain instead of more natural movement among the skin, fat, and muscle tissues so that large and/or stronger relative movements exist among them. Therefore, it is desirable to relieve or minimize skin strain. Reducing the gel thickness to increase flexibility can partially improve the situation. We found that an alternative approach is to cut a large electrode into smaller ones and connect them as a new electrode, that is, make an electrode array [Fig. 5(b)]. Clearly, the results suggest that the SAR does not increase for a simple increase in area, but does increase if a large area electrode is constructed from a group of small electrodes. Furthermore, it is beneficial for this application to carve some holes and slots in a sticky electrode so that it is more flexible to movement.

Fig. 6 shows the results when the electrode array method was used to increase the size of the Siemens Burdick Signa II. Based on our experiments, a small electrode is sensitive to location and occasionally has high SAR for some specific placement, but it is difficult to relocate it exactly to always obtain high SAR. As shown in Fig. 6, most small electrodes have low SAR. To achieve large effective area an electrode should have a metal film over

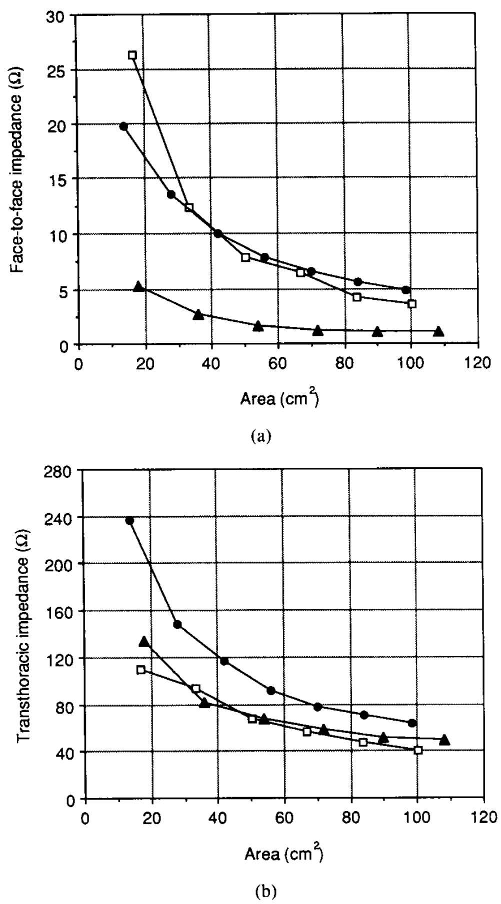

Fig. 4. Impedance decreases as area increases. (a) Face-to-face impedances. (b) Transthoracic-plus-electrode impedances. The decrease in ohms is larger for transthoracic-plus-electrode impedance. Symbols: ●, Siemens Burdick Signa II; □, Sentry Rubber; ▲, Marquette defibrillator.

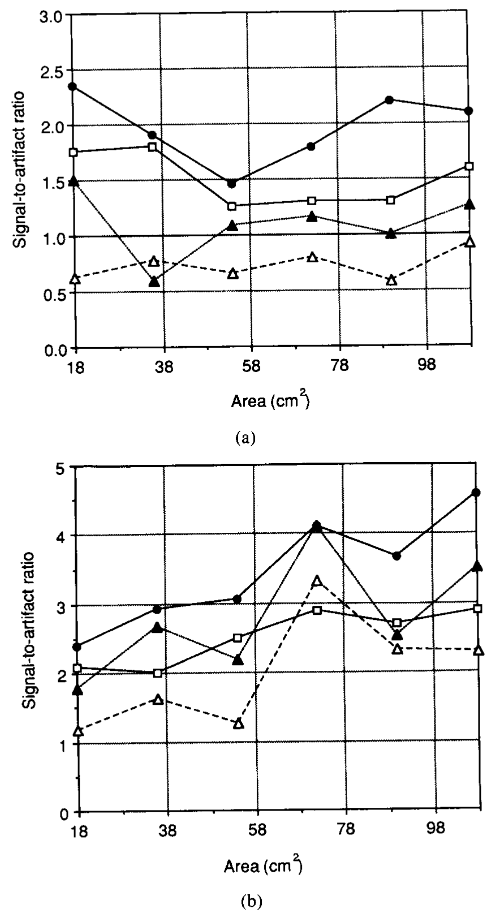

Fig. 5. Signal-to-artifact ratio for chest and abdominal breathing as a function of area. (a) SAR for the Marquette defibrillator 400317-001 electrodes does not increase for a simple increase in area. (b) SAR increases when connecting two or more 18-cm^2 pieces cut from the electrode to construct a new electrode with a larger area. Symbols: □, for chest breathing on subject 1; ●, for abdominal breathing on subject 1; △, for chest breathing on subject 2; ▲, for abdominal breathing on subject 2.

the entire back so that the effective area of the electrode is large. An ECG electrode with rather small effective area and with a large insulated disk ring for adhesion, like Dispos-A-Trode/2, should be avoided. Also, a large adhesive disk introduces additional artifacts.

An interesting question is how big an electrode should be. Figs. 5 and 6 show that, at least for one location, a peak SAR occurs at around 70 cm^2 for adults. A possible explanation is that an electrode averages the signals under it. However, the signal amplitude decreases for large area. Thus, the SAR of a large electrode would be lower than that of a smaller one. From Fig. 6 we cannot conclude that 70 cm^2 is an optimal size for all locations. But it implies that at a particular area which achieves a peak SAR, a local optimal size exists for the particular location.

C. Electrode Placements

The previous study on electrode sizes shows that large area electrodes have large SAR's. But for the study on electrode placements, to prevent spatial averaging requires small electrodes. Based on Fig. 6, we compromised by connecting two Signa IIs (each 7 cm^2) as a 14 cm^2 electrode and soldered a connecting wire between them.

Tables II–VII list the SAR's for the worst case, the best case, mean and standard deviation of normalized SAR for 171 locations from ten subjects. The best location would have the highest SAR from all combinations for all subjects. Although no location completely satisfies the condition, we can still find some good choices for our application.

Of all the 171 combinations, electrode-pair location 19–0 provided the highest SAR's for both the worst case and mean of the normalized value. The next best combinations include electrode-pair locations 19–10, 31–6, 3–0 and 3–21. For a ventilation measurement system or an

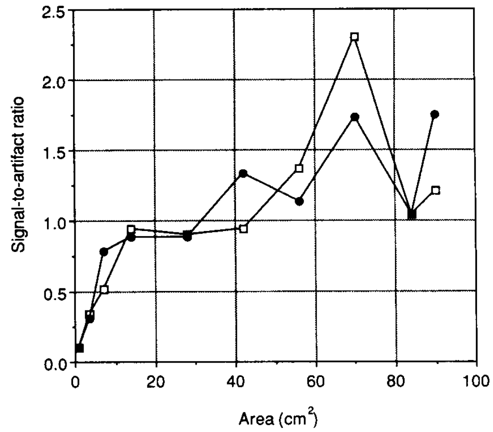

Fig. 6. Signal-to-artifact ratio for the Siemens Burdick Signa II electrodes increases when connecting two or more 7-cm^2 Signa IIs to construct a new electrode with a larger area. Note a peak SAR exists around 70 cm^2. Symbols: □, for chest breathing; ●, for abdominal breathing.

TABLE II
THE SAR'S USING LOCATION 0 AS REFERENCE PLACEMENT

Electrode-Pair Location Number	SAR (The worst case)	SAR (The best case)	Mean of the Normalized SAR	Standard Deviation of the Normalized SAR
1-0	0.04	0.22	0.15	0.06
2-0	0.04	0.38	0.12	0.05
3-0	0.17	0.50	0.38	0.19
4-0	0.04	0.25	0.17	0.13
5-0	0.12	0.45	0.30	0.14
6-0	0.07	0.75	0.35	0.23
7-0	0.13	0.33	0.27	0.11
8-0	0.11	0.45	0.29	0.10
9-0	0.13	0.43	0.26	0.11
10-0	0.07	0.44	0.22	0.15
11-0	0.02	0.44	0.15	0.10
12-0	0.13	0.46	0.29	0.11
13-0	0.08	0.36	0.25	0.11
14-0	0.01	0.18	0.12	0.12
15-0	0.02	0.17	0.15	0.08
16-0	0.05	1.33	0.23	0.18
17-0	0.03	0.43	0.16	0.07
18-0	0.11	0.45	0.32	0.21
19-0	0.19	0.64	0.57	0.28
20-0	0.13	0.50	0.42	0.17
21-0	0.06	0.57	0.30	0.18
22-0	0.11	0.44	0.31	0.10
23-0	0.07	0.38	0.24	0.17
24-0	0.02	0.63	0.27	0.19
25-0	0.08	0.50	0.28	0.17
26-0	0.03	0.46	0.18	0.09
27-0	0.08	0.38	0.23	0.13
28-0	0.13	0.40	0.33	0.15
29-0	0.02	0.17	0.12	0.12
30-0	0.06	0.26	0.21	0.12
31-0	0.04	0.37	0.30	0.22

apnea monitor which uses only two electrodes, therefore, our data suggest that we place two electrodes on Locations 0 and 19. For multiple electrode measurement, attempts to improve the performance of an impedance-based monitor could place electrode pairs in locations 31-6, 19-10, 3-0 and 3-21. In contrast, electrode-pair location 29-25, placed on the upper and lower positions of the rib cage edge on the midaxillary line of one side gave the lowest SAR for both the worst case and mean of the normalized value. This combination may be useful to detect motion

TABLE III
THE SAR'S USING LOCATION 31 AS REFERENCE PLACEMENT

Electrode-Pair Location Number	SAR (The worst case)	SAR (The best case)	Mean of the Normalized SAR	Standard Deviation of the Normalized SAR
1–31	0.04	0.27	0.21	0.15
2–31	0.03	0.42	0.17	0.12
3–31	0.05	0.35	0.28	0.17
4–31	0.03	0.53	0.33	0.27
5–31	0.05	0.58	0.33	0.18
6–31	0.17	1.00	0.41	0.11
7–31	0.05	0.29	0.25	0.15
8–31	0.07	0.64	0.35	0.22
9–31	0.04	0.62	0.32	0.25
10–31	0.06	1.11	0.31	0.25
11–31	0.03	0.67	0.23	0.12
12–31	0.05	0.80	0.50	0.32
13–31	0.07	0.78	0.38	0.23
14–31	0.03	0.33	0.30	0.20
15–31	0.07	0.36	0.29	0.21
16–31	0.05	0.31	0.23	0.13
17–31	0.05	0.34	0.21	0.09
18–31	0.03	0.30	0.27	0.19
19–31	0.02	0.40	0.41	0.29
20–31	0.02	0.39	0.30	0.18
21–31	0.05	0.49	0.31	0.16
22–31	0.05	0.39	0.30	0.20
23–31	0.05	0.35	0.21	0.10
24–31	0.04	0.54	0.31	0.20
25–31	0.06	0.82	0.30	0.17
26–31	0.04	0.53	0.24	0.11
27–31	0.01	0.23	0.10	0.06
28–31	0.08	0.71	0.39	0.29
29–31	0.06	0.40	0.26	0.18
30–31	0.05	0.63	0.33	0.24

TABLE IV
THE SAR'S USING LOCATION 21 AS REFERENCE PLACEMENT

Electrode-Pair Location Number	SAR (The worst case)	SAR (The best case)	Mean of the Normalized SAR	Standard Deviation of the Normalized SAR
1–21	0.05	1.50	0.29	0.19
2–21	0.04	0.57	0.23	0.12
3–21	0.13	0.70	0.34	0.12
4–21	0.08	1.36	0.43	0.23
5–21	0.05	1.33	0.44	0.19
6–21	0.05	1.25	0.45	0.22
7–21	0.03	0.50	0.26	0.12
8–21	0.01	0.71	0.35	0.28
9–21	0.01	0.88	0.36	0.24
10–21	0.03	1.40	0.38	0.26
11–21	0.03	0.82	0.26	0.14
12–21	0.02	0.80	0.37	0.25
13–21	0.01	0.90	0.31	0.18
14–21	0.03	0.88	0.23	0.13
15–21	0.01	0.57	0.22	0.11
16–21	0.01	1.33	0.19	0.19
17–21	0.01	0.55	0.10	0.07
18–21	0.08	0.31	0.23	0.11
19–21	0.09	0.57	0.41	0.18
20–21	0.04	1.00	0.28	0.15
22–21	0.04	0.50	0.29	0.16
23–21	0.02	1.50	0.28	0.21
24–21	0.02	0.67	0.29	0.19
25–21	0.01	0.60	0.19	0.13
26–21	0.02	1.00	0.24	0.16
27–21	0.02	0.80	0.31	0.17
28–21	0.01	1.00	0.31	0.22
29–21	0.02	0.75	0.23	0.28
30–21	0.05	0.54	0.26	0.18

TABLE V
THE SAR'S USING LOCATION 25 AS REFERENCE PLACEMENT

Electrode-Pair Location Number	SAR (The worst case)	SAR (The best case)	Mean of the Normalized SAR	Standard Deviation of the Normalized SAR
1–25	0.01	0.47	0.18	0.14
2–25	0.02	0.41	0.14	0.06
3–25	0.06	0.70	0.30	0.14
4–25	0.02	0.27	0.21	0.11
5–25	0.01	0.56	0.26	0.13
6–25	0.01	0.90	0.31	0.15
7–25	0.04	0.58	0.25	0.10
8–25	0.03	0.75	0.31	0.28
9–25	0.04	1.00	0.23	0.14
10–25	0.02	1.00	0.25	0.16
11–25	0.05	0.75	0.19	0.11
12–25	0.03	0.78	0.26	0.28
13–25	0.06	0.80	0.2	0.10
14–25	0.02	0.38	0.11	0.07
15–25	0.03	0.20	0.13	0.06
16–25	0.01	0.80	0.16	0.10
17–25	0.01	0.64	0.15	0.09
18–25	0.07	0.36	0.22	0.08
19–25	0.06	0.50	0.39	0.21
20–25	0.02	0.44	0.16	0.08
22–25	0.02	0.44	0.25	0.11
23–25	0.07	0.83	0.24	0.10
24–25	0.01	1.00	0.26	0.15
26–25	0.04	0.57	0.18	0.09
27–25	0.01	0.50	0.26	0.16
28–25	0.01	0.60	0.18	0.11
29–25	0.01	0.09	0.05	0.04
30–25	0.01	0.38	0.14	0.09

TABLE VI
THE SAR'S USING LOCATION 6 AS REFERENCE PLACEMENT

Electrode-Pair Location Number	SAR (The worst case)	SAR (The best case)	Mean of the Normalized SAR	Standard Deviation of the Normalized SAR
1–6	0.02	0.50	0.17	0.09
2–6	0.01	0.29	0.11	0.06
3–6	0.06	0.70	0.32	0.17
4–6	0.04	1.00	0.43	0.18
5–6	0.04	2.00	0.45	0.28
7–6	0.04	0.75	0.32	0.17
8–6	0.01	1.25	0.46	0.27
9–6	0.01	1.00	0.33	0.17
10–6	0.05	0.38	0.24	0.11
11–6	0.01	0.64	0.25	0.12
12–6	0.01	0.91	0.44	0.20
13–6	0.01	0.78	0.31	0.16
14–6	0.02	0.42	0.20	0.12
15–6	0.02	0.57	0.25	0.10
16–6	0.05	1.33	0.32	0.16
17–6	0.04	1.00	0.31	0.16
18–6	0.07	0.57	0.38	0.21
19–6	0.09	0.67	0.49	0.21
20–6	0.06	1.20	0.47	0.18
22–6	0.09	0.80	0.36	0.10
23–6	0.06	1.00	0.37	0.14
24–6	0.02	1.19	0.42	0.18
26–6	0.06	1.20	0.35	0.15
27–6	0.09	1.00	0.39	0.20
28–6	0.01	1.07	0.51	0.27
29–6	0.01	0.42	0.26	0.14
30–6	0.13	0.64	0.31	0.11

TABLE VII
THE SAR'S USING LOCATION 10 AS REFERENCE PLACEMENT

Electrode-Pair Location Number	SAR (The worst case)	SAR (The best case)	Mean of the Normalized SAR	Standard Deviation of the Normalized SAR
1-10	0.03	0.32	0.14	0.14
2-10	0.03	0.63	0.13	0.11
3-10	0.07	1.67	0.30	0.08
4-10	0.04	0.78	0.32	0.24
5-10	0.08	0.88	0.29	0.20
7-10	0.07	0.83	0.23	0.08
8-10	0.06	1.00	0.25	0.10
9-10	0.02	0.80	0.23	0.12
11-10	0.02	0.57	0.22	0.14
12-10	0.03	0.73	0.22	0.12
13-10	0.08	0.40	0.18	0.07
14-10	0.01	0.17	0.06	0.04
15-10	0.06	0.36	0.13	0.05
16-10	0.05	2.00	0.26	0.27
17-10	0.04	1.80	0.24	0.24
18-10	0.11	0.90	0.30	0.11
19-10	0.14	0.61	0.36	0.14
20-10	0.04	0.42	0.33	0.17
22-10	0.06	0.83	0.32	0.10
23-10	0.05	0.63	0.23	0.09
24-10	0.03	1.00	0.26	0.15
26-10	0.01	0.75	0.22	0.12
27-10	0.02	0.83	0.32	0.18
28-10	0.02	0.63	0.22	0.10
29-10	0.01	0.36	0.13	0.08
30-10	0.02	0.32	0.21	0.14

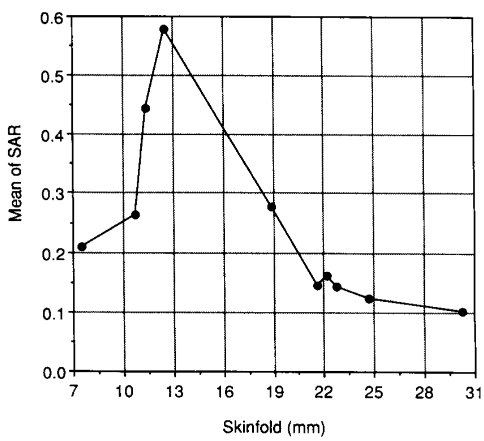

Fig. 7. The thickness of skinfold influences the mean value of the SAR. Every mean is an average of 171 SAR's from each subject. The skinfold value is the averaged thickness of chest and abdominal skinfolds. Measurements refer to [10].

signals if desired. The next worst placements are electrode-pair location 14–10, a symmetric position, as well as 2–6 and 17–21.

In addition, we note a relationship between SAR values and fat or lean subjects. Higher SARs were obtained from subjects with less fat tissue (Fig. 7).

Further data are required to determine the relationship between SAR and electrode area for electrode-pair locations 19–0.

ACKNOWLEDGMENT

We thank R. Zhou and K. P. Cohen for their cooperations and all the volunteers for their assistance in this study. We also thank Siemens Burdick, Inc. for contributing electrodes for use in this study.

APPENDIX
TEST PROTOCOL

We have developed several protocols to test the abilities of a ventilation measurement system to distinguish among situations of normal ventilation, abnormal ventilation, movement during normal ventilation, and movement during abnormal ventilation. The following is one of them for comparing electrode types, sizes, and placements under the same test conditions.

A. *Tidal Breathing Acquisition*

This protocol is for recording natural breathing, including shallow breathing.

The subject lies supine on a mattress in a quiet environment (room temperature 28°C) and with an orientation so that he or she cannot see the computer or operators. Unless instructed to do otherwise, the subject 1) keeps quiet, relaxes and breathes naturally, and 2) minimizes body movement. Simultaneously, the operator observes the impedance signals to check whether the subject has relaxed and begun natural breathing. After waiting for several minutes, the operator quietly starts the recorder so that the subject is not aware when the recording begins.

B. Chest Breathing

Lying supine, the subject breathes normally using the chest muscles and minimizes movement of the abdomen.

C. Abdominal Breathing

Lying supine, the subject breathes normally using abdominal muscles and minimizes movement of the chest.

D. Movement Maneuvers

1) Limb Movement: From the initial position, lying supine, put two hands over your head and touch the bed. The angle between the upper arm and lower arm is about 120°. Maintain the angle during the motion. Stretch legs out on the bed.

Raise all four limbs from the initial position until two hands touch the two sides near the buttocks on the bed, and the thighs are about 90° with respect to body and the knee included angle is about 60°. The two hands have made 180° arc curves in space.

Then reverse the above process to move the limbs back to the initial position to complete one cycle.

2) Body Rotation: Starting from the supine position, turn onto left side within 1.8 s, stay on side for 1 s, then turn back to supine position within 1.8 s. Stay supine for 1 s.

Next, repeat the process turning onto the right side to complete one cycle.

E. Motion Artifact Acquisition

After recording tidal breathing for 1.7 min, chest breathing and abdominal breathing for 1.3 min respectively, the operator starts the periodic beep signal, asks the subject to stop breathing and to synchronize with the beep or counter sign, moving limbs for four cycles. Then start natural breathing again to finish segment.

After about four natural breathing cycles, the subject repeats the same limb movement.

After another four natural breathing cycles, the subject rotates the body once.

F. Calculating the SAR

The signal-to-artifact ratio (SAR) for normal breathing is obtained by measuring the minimal value of the peak-to-peak cycle of the tidal breathing and the maximal peak-to-peak value of motion.

The SAR for chest breathing is obtained by measuring the minimal value of the peak-to-peak cycle of the chest breathing and the maximal peak-to-peak value of motion.

The SAR for abdominal breathing is obtained by measuring the minimal value of the peak-to-peak cycle of the abdominal breathing and the maximal peak-to-peak value of motion.

References

[1] *Apnea Monitoring by Means of Thoracic Impedance Pneumography* (AAMI TIR No. 4-1989). Association for the Advancement of Medical Instrumentation (AAMI), 3330 Washington Boulevard, Suite 400, Arlington, VA 22201-4598, 1989.

[2] J. G. Webster, Ed., *Electrical Impedance Tomography*. Bristol, England: Adam Hilger, 1990.

[3] D. Warburton, A. R. Stark, and H. W. Taeusch, "Apnea monitor failure in infants with upper airway obstruction," *Pediatrics*, vol. 60, pp. 742–744, 1977.

[4] L. Black, L. Hersher and A. Steinschneider, "Impact of the apnea monitor on family life," *Pediatrics*, vol. 62, pp. 681–685, 1978.

[5] National Institute of Health Consensus Development Conference, "Infantile apnea and home monitoring," *Pediatrics*, vol. 79, pp. 292–299, 1987.

[6] A. V. Sahakian, W. J. Tompkins, and J. G. Webster, "Electrode motion artifacts in electrical impedance pneumography," *IEEE Trans. Biomed. Eng.*, vol. BME-32, pp. 448-451, 1985.

[7] D. J. Nowicki and J. G. Webster, "A one op-amp current source for electrical impedance tomography," in *Proc. Annu. Int. Conf. IEEE Eng. Med. Biol. Soc.*, 1989, vol. 11, pp. 455–456.

[8] M. R. Akbarzadeh, W. J. Tompkins, and J. G. Webster, "Multichannel impedance pneumography for apnea monitoring," in *Proc. Annu. Int. Conf. IEEE Eng. Med. Biol. Soc.*, 1990, vol. 12, pp. 1048–1049.

[9] P. Hua, E. J. Woo, W. J. Tompkins, and J. G. Webster, "An electrical impedance tomograph using compound electrodes," in *Proc. Annu. Int. Conf. IEEE Eng. Med. Biol. Soc.*, 1989, vol. 11, pp. 472–473.

[10] R. A. Oppliger and R. R. Clark, *Handbook for Standardizing Skinfold Measurements and Calculating Minimum Weight for the Wisconsin Wrestling Minimum Weight Project*, Wisconsin Interscholastic Athletic Association, 41 Parkridge Dr., P.O. Box 267, Stevens Point, WI 54481-0267, 1991.

Shen Luo (S'92) received the B.E.E. degree and M.S.E.E. degree from Huazhong University of Science and Technology, Wuhan, China, in 1982 and 1985, respectively.

From 1985 to 1988, he was a faculty member in the Department of Automatic Control Engineering of Huazhong University of Science and Technology, Wuhan, China, where he taught and did research on microcomputer-based instrumentation. He is currently working towards the Ph.D. degree in electrical engineering at the University of Wisconsin-Madison. His research interests include electrodes and algorithms for impedance-based ventilation systems, high-resolution cardiac signals including alignment methods, and electrocardiogram (ECG) to vectorcardiogram (VCG) transformation.

Valtino X. Afonso (S'91) received the B.S. degree in electrical and computer engineering from Marquette University, Milwaukee, WI, in 1990.

He is presently doing graduate work at the University of Wisconsin, Madison, and is pursuing the M.S. and Ph.D. degrees. His research interests include the application of signal processing to biomedical problems.

Mr. Afonso is a member of Tau Beta Pi.

John G. Webster (M'59–SM'69–F'86) received the B.E.E. degree from Cornell University, Ithaca, NY, in 1953, and the M.S.E.E. and Ph.D. degrees from the University of Rochester, Rochester, NY, in 1965 and 1967, respectively.

He is Professor of Electrical and Computer Engineering at the University of Wisconsin-Madison. In the field of medical instrumentation he teaches undergraduate, graduate, and short courses, and does research on electrical impedance tomography, tactile sensors, electrodes, and biopotential amplifiers. He is author of *Transducers and Sensors*—an IEEE/EAB Individual Learning Program (Piscataway, NJ: IEEE, 1989). He is coauthor with B. Jacobson of *Medicine and Clinical Engineering* (Englewood Cliffs, NJ: Prentice-Hall, 1977), and with R. Pallás-Areny of *Sensors and Signal Conditioning* (New York: Wiley, 1991). He is editor of *Encyclopedia of Medical Devices and Instrumentation* (New York: Wiley, 1988), *Tactile Sensors for Robotics and Medicine* (New York: Wiley, 1988), *Electrical Impedance Tomography* (Bristol, England: Adam Hilger, 1990), *Teaching Design in Electrical Engineering* (Piscataway, NJ: Educational Activities Board, IEEE, 1990), *Prevention of Pressure Sores: Engineering and Clinical Aspects* (Bristol, England: Adam Hilger, 1991), and *Medical Instrumentation: Application and Design, 2nd ed.* (Boston: Houghton Mifflin, 1992). He is coeditor with A.M. Cook of *Clinical Engineering: Principles and Practices* (Englewood Cliffs, NJ: Prentice-Hall, 1979) and *Therapeutic Medical Devices: Application and Design* (Englewood Cliffs, NJ: Prentice-Hall, 1982); with W. J. Tompkins of *Design of Microcomputer-Based Medical Instrumentation* (Englewood Cliffs, NJ: Prentice-Hall, 1981) and *Interfacing Sensors to the IBM PC* (Englewood Cliffs, NJ: Prentice Hall, 1988); and with A. M. Cook, W. J. Tompkins, and G. C. Vanderheiden of *Electronic Devices for Rehabilitation* (London: Chapman & Hall, 1985).

Dr. Webster has been a member of the IEEE-EMBS Administrative Committee and the NIH Surgery and Bioengineering Study Section. He has been Associate Editor, Medical Instrumentation, of the IEEE Transactions on Biomedical Engineering, and Chairman of the IEEE-EMBS Fellow Committee. He is a fellow of the American Institute of Medical and Biological Engineering.

Willis J. Tompkins (S'61–M'66–SM'77–F'92) received the B.S. and M.S. degrees in electrical engineering from the University of Maine, Orono, in 1963 and 1965, respectively, and the Ph.D. degree in biomedical electronic engineering from the University of Pennsylvania, Philadelphia, in 1973.

From 1965 to 1968, he was an electrical engineer at Sanders Associates, Inc., Nashua, NH, where he worked on research and development of data storage systems. He was employed from 1973 to 1974 at the Hospital of the University of Pennsylvania as a biomedical engineer. Since 1974, he has been on the faculty of the University of Wisconsin-Madison. Currently Professor of Electrical and Computer Engineering, he teaches undergraduate, graduate, and short courses on the topic of computers in medicine. His research interests include applications of microcomputer-based medical instrumentation and on-line biomedical computing. He is coeditor with J. G. Webster of the Prentice-Hall textbooks, *Design of Microcomputer-Based Medical Instrumentation* (Englewood Cliffs, NJ: Prentice-Hall, 1981) and *Interfacing Sensors to the IBM PC* (Englewood Cliffs, NJ: Prentice-Hall, 1988). He is coeditor with J. G. Webster, A. M. Cook, and G. C. Vanderheiden of the textbook, *Electronic Devices for Rehabilitation* (New York: Wiley, 1985).

Dr. Tompkins is a past President of the IEEE Engineering in Medicine and Biology Society. He is also a member the IEEE Computer Society, the Association for the Advancement of Medical Instrumentation, the Biomedical Engineering Society, and the American Society for Engineering Education. He is a Fellow of the American Institute for Medical and Biological Engineering. He is a Registered Professional Engineer in Wisconsin.